The intricate details of the initial flaw shape can be ignored in the first approximation, expecially since, upon incipient growth, the crack rapidly attains a stable configuration (normally semicircular, semielliptic, etc., depending on the stress distribution).

Figure 3 shows an extrapolation of the macroscopic crack length record, $a=f(N)$, over the life span preceding the macroscopic observations, down to a semicircular initial flaw length shown at the start of the cycling curve. Note that this is merely for illustration as the extrapolated X axis in Fig. 3 is not to scale. A median curve drawn through the macroscopic crack growth record, $a=f(N)$ with $a>0.1$ in., was differentiated graphically yielding $da/dN=f_1(a)=f_2(\Delta K)$, which can be plotted against the corresponding ΔK levels given by

$$\Delta K=\Delta\sigma\sqrt{\pi a} \tag{1}$$

Acknowledgments

Tests were performed by J.F. Smith Jr., Analyst; and consultation was given by J. Miller, Senior Engineer, Experimental Mechanics Lab, G.E.-AEG, Lynn, Mass.

AIAA 81-4192

Radar Ranges for Carrier-Based AEW Aircraft

Ralph R. Nebiker*
Carrier Airborne Early Warning Squadron 115, U.S. Navy, San Francisco, Calif.

Introduction

THIS Note describes a simple geometrical model that may be used to examine the affects of various parameters on the minimum required radar range for carrier-based airborne early warning (AEW) aircraft. The motivation for this Note was the work described in Ref. 1, which examined the AEW aircraft in a coastal defense role. Here the development and results are focused on the geometry of an aircraft carrier battle group (BG) at sea (airbase and target colocated), the standoff weapon capability of enemy air-to-surface antiship missiles, and two BG response options with deck-launched interceptors (DLI) and barrier combat air patrol (BARCAP) prepositioned on station.

Model Development

Figure 1 depicts the basic scenario with the BG at point A and the AEW aircraft at point B. Continuation of line AB forms the threat reference axis (TRA) from which significant angles are measured. Attacking fighters need arrive only within distance L_1 (the lethal range of their air-to-air weapons) of the AEW aircraft, and attacking bombers need arrive only within distance W (launch range of their antiship missiles) of the BG. The objective is to destroy the bombers before they launch their missiles. The BG commander can, in response, launch DLI from point A or provide BARCAP on station at point G. The DLI and BARCAP are equipped with air-to-air weapons of range L_2 and fly at velocity V_4. If the AEW aircraft pilot decides after a time T_1 that he is under attack by enemy fighters, he flees toward point A at velocity V_3. The BARCAP is assigned a similar maneuver and decision delay time of T_2.

Figure 2 (top) depicts the geometry of a BARCAP interdicting a bomber attack. Let J denote the desired intercept point on the straight-line path AL of the attacking bombers, $X=$ distance AJ. With $T=$ the time to engagement,

$$V_4\cdot(T-T_2)+L_2=GJ$$

By the law of cosines

$$GJ^2=S^2+X^2-2\cdot S\cdot X\cdot\cos(A_3-A_2)$$

and

$$T=\frac{[S^2+X^2-2\cdot S\cdot X\cdot\cos(A_3-A_2)]^{1/2}+V_4\cdot T_2-L_2}{V_4} \tag{1}$$

If $|(A_3-A_2)|$ is less than 90 deg *and* W is less than $S\cdot\cos(A_3-A_2)$, then the shortest route to interdiction is GJ perpendicular to AL, where $X=S\cdot\cos(A_3-A_2)$; otherwise, $X=W$. To insure sufficient time for intercept $AL=V_1\cdot T+X$ and from triangle ABL, where $BL=R$, the required radar range,

$$D\cdot\cos(A_3)+R\cdot\cos(A_4)=V_1\cdot T+X \tag{2}$$

Triangles ABK and LBK yield

$$\sin(A_4)=(D/R)\cdot\sin(A_3)$$

Since $\cos^2+\sin^2=1$, $\cos^2(A_4)=1-(D^2/R^2)\cdot\sin^2(A_3)$. Substituting into Eq. (2) and solving for R leads to

$$R=\{[X+V_1\cdot T-D\cdot\cos(A_3)]^2+D^2\cdot\sin^2(A_3)\}^{1/2} \tag{3}$$

where T is obtained from Eq. (1).

The geometry of a BARCAP response to a fighter attack on the AEW aircraft is depicted in Fig. 2 (bottom). Using the law of cosines for triangle ABG yields

$$GB^2=D^2+S^2-2\cdot D\cdot S\cdot\cos(A_2) \tag{4}$$

Triangles ABE and CBE provide the following relations:

$$A_5=\arcsin(D\cdot\sin(A_1)/R) \tag{5}$$

$$AC=D\cdot\cos(A_1)+R\cdot\cos(A_5) \tag{6}$$

$$CF=AC-S\cdot\cos(A_2-A_1) \tag{7}$$

Triangles AGF and CGF lead to

$$A_6=\arctan(S\cdot\sin(A_2-A_1)/\mathrm{CF}) \tag{8}$$

$$GC=CF/\cos(A_6) \tag{9}$$

Applying the law of cosines to triangle CBG yields

$$A_7=\arccos\left(\frac{R^2+GB^2-GC^2}{2\cdot GB\cdot R}\right) \tag{10}$$

Let H denote the desired intercept point along the straight-line intercept path CB of the attacking fighter, $X=$ distance BH. If $|A_7|$ is less than 90 deg *and* L_1 is less than $GB\cdot\cos(A_7)$, then the shortest route to interdiction is GH perpendicular to CB, where $X=GB\cdot\cos(A_7)$; otherwise $X=L_1$.

From triangle GBH and the law of cosines

$$GH=[GB^2+X^2-2\cdot GB\cdot X\cdot\cos(A_7)]^{1/2} \tag{11}$$

Received Oct. 6, 1980; revision received Dec. 22, 1980.

*Operations Officer, Commander, VAW-115. Member AIAA.

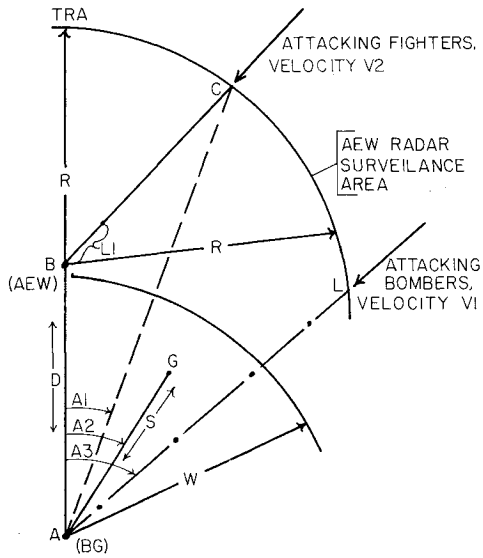

Fig. 1 Basic scenario of carrier-based AEW radar surveillance problem.

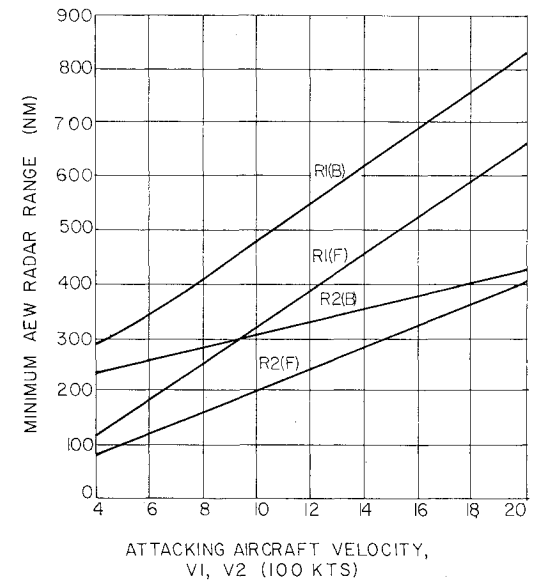

Fig. 3 Minimum AEW radar range as function of attacking bomber and fighter velocities, based on scenario 1 parameters (see Table 1).

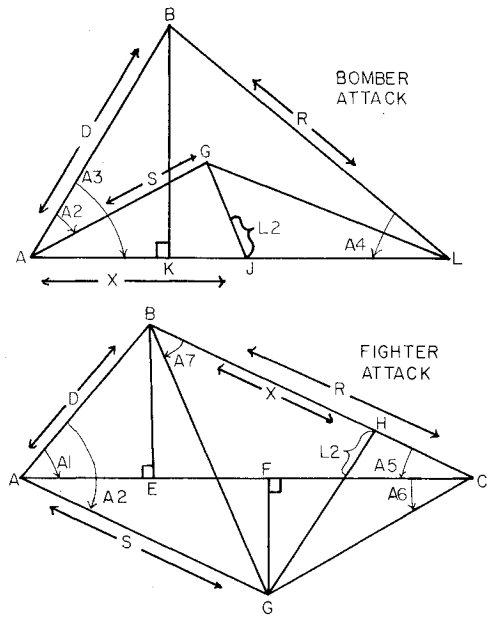

Fig. 2 Interdiction geometry of BARCAP response to a bomber attack (top) and a fighter attack (bottom).

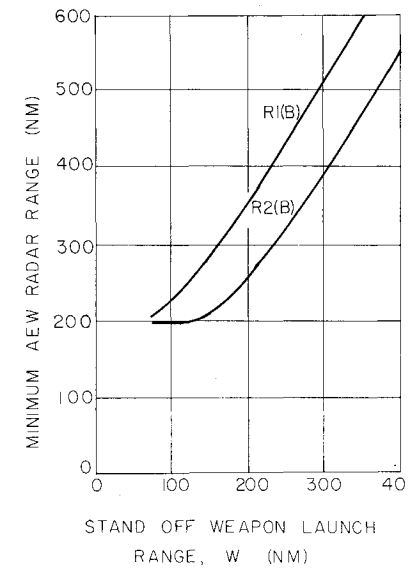

Fig. 4 Minimum AEW radar range as a function of standoff weapon launch range, based on scenario 1 parameters (see Table 1).

Table 1 AEW radar ranges

Parameter	Scenario 1	2	3	4	5
V_1 (bomber velocity), knot	600.0	600.0	600.0	450.0	450.0
V_2 (fighter velocity), knot	600.0	600.0	600.0	450.0	450.0
V_3 (AEW velocity), knot	200.0	200.0	200.0	200.0	200.0
V_4 (BARCAP and DLI velocity), knot	800.0	800.0	800.0	550.0	600.0
A_1, deg	20.0	45.0	45.0	40.0	45.0
A_2, deg	40.0	20.0	20.0	20.0	20.0
A_3, deg	60.0	45.0	45.0	60.0	45.0
W, n.mi.	200.0	200.0	160.0	160.0	160.0
S (BARCAP/DLI), n.mi.	120/0	120/0	120/0	120/0	120/0
D, n.mi.	220.0	220.0	140.0	180.0	180.0
L_1, n.mi.	25.0	25.0	25.0	25.0	25.0
L_2, n.mi.	50.0	50.0	50.0	50.0	50.0
T_1, min	5.0	5.0	5.0	5.0	5.0
T_2 (BARCAP/DLI), min	5/10	5/10	5/10	5/10	5/10
R_1 (F), n.mi.	188.3	215.9	167.0	162.8	165.0
R_1 (B), n.mi.	357.3	300.3	262.8	282.0	228.8
R_2 (F), n.mi.	125.2	156.1	99.7	119.5	133.9
R_2 (B), n.mi.	258.5	206.1	161.4	216.8	154.0

Thus T, the time to engagement, is

$$T=(GH+V_4\cdot T_2-L_2)/V_4 \tag{12}$$

The time to engagement for the attacking fighter T' must equal T to insure interdiction, where

$$T'=(R-X)/V_2 \tag{13}$$

Because of the trigonometric functions involved in the computations, the function

$$f(R')=T-T' \tag{14}$$

was formed and solved for R' by the regular falsi method[2] using a Wang 2200 to perform the repetitive calculations. Equations (4-14) were computed in turn for each pass. Since the AEW aircraft flees toward point A, the above calculations were computed within a loop of successive values of $D=D'$, formed by

$$D_i'=D-V_3\cdot(T_i-T_1) \tag{15}$$

where T_i is obtained from Eq. (12). Computations ceased when successive values of D' differed by less than 1 mile

$$|D_{i+1}'-D_i'|<=1.0 \tag{16}$$

Both Eqs. (14) and (16) are smooth valued and well formed in the region of interest: T greater than T_2. Following final solution of Eq. (14) the required radar range R was calculated by the law of cosines from triangle ABC

$$R=[D^2+AC^2-2\cdot D\cdot AC\cdot\cos(A_1)]^{1/2} \tag{17}$$

The DLI response is obtained by setting S (BARCAP station range) equal to zero, T_2 is then the DLI alert status. For the DLI response the solution to Eq. (3) is denoted by R_1(B), indicating a DLI response (R_1) to a bomber (B) attack. Similarly the solution to Eq. (17) is represented by R_1(F), indicating a DLI response to a fighter attack (F). R_2(B) and R_2(F) represent solutions to Eqs. (3) and (17), respectively, indicating a BARCAP response (R_2) to the same type of attack.

Results

In spite of the differences in geometry between this Note and that of Ref. 1, there is considerable agreement in the general trend and direction of comparable parameters. The most significant difference is in the relationship between the AEW radar range and the attacking fighter's velocity. Reference 1 indicates a concave downward function for the DLI comparable solution. This would imply that at some point the required radar range would reach a maximum and then decrease for even greater values of attacking fighter velocity. The present case (Fig. 3) indicates a monotonically increasing function for both the DLI and BARCAP response, as would be expected.

In the majority of scenarios examined by the author (Table 1), the three most significant factors requiring the largest minimum radar ranges were attacking fighter velocity, attacking bomber velocity, and standoff weapon launch range. Figures 3 and 4 depict these parameters and clearly indicate the DLI response is of major importance in minimum radar range design requirements.

References

[1] Bracken, J. and Grotte, J.H., "Required Radar Ranges for AEW Aircraft," *Journal of Aircraft*, Vol. 16, Nov. 1979, pp. 792-797.

[2] Kreyszig, E., *Advanced Engineering Mathematics*, 2nd Ed., John Wiley and Sons, New York, 1967.

AIAA 81-4193

A Geometrical Study of the Steady-State Spin for a Typical Low-Wing General Aviation Aircraft

Andrew P. Imbrie*
Princeton University, Princeton, N.J.

Introduction

In a fully evolved spin, the aircraft's center of gravity (c.g.) follows a descending helical path about the spin axis. This Note pertains to the aircraft's orientation relative to that helix, as well as the geometric and kinematic effects of the spin on the local velocity vector. Using flight test data for a low-wing general aviation aircraft,[1] this Note presents results pertaining to aircraft orientation, flow patterns, and the aerodynamic driving mechanisms in a steady-state spin.

The Kinematic Equations

It is assumed that the aircraft is in a steady-state spin with spin rate Ω, spin radius R_s, vertical velocity $w_{c.g.}$, and Euler attitude angles θ, ϕ, and $\psi-\eta$ given (Fig. 1). Coordinates of the aircraft's configuration are referred to the c.g. location along the conventional Cartesian system (x, y, and z). Referring to Fig. 1, it can be shown[2] that the orthogonal body-axis velocity components of any point p on the aircraft

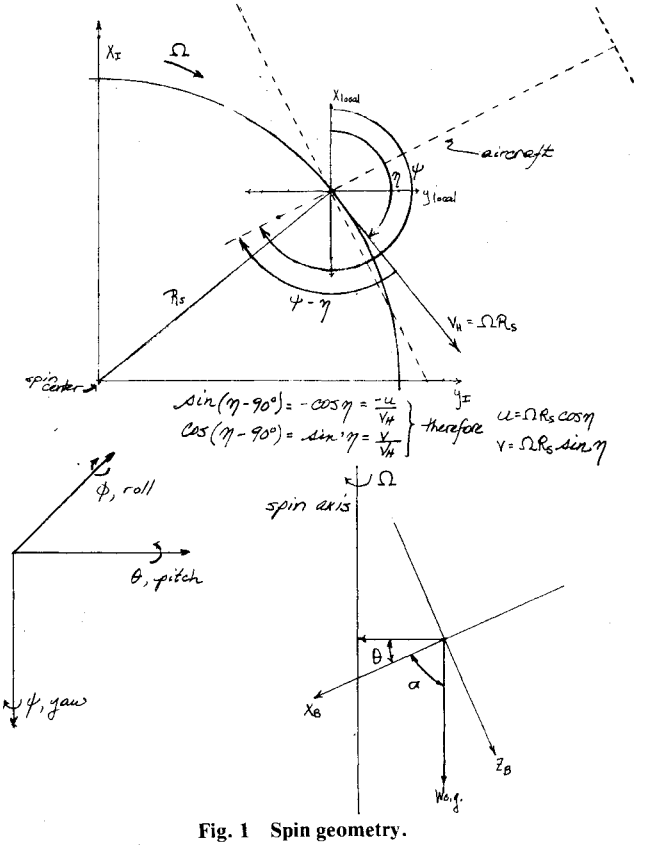

Fig. 1 Spin geometry.

Received Oct. 21, 1980; revision received Jan. 15, 1981.

*Undergraduate Student, Department of Mechanical and Aeronautical Engineering; currently Graduate Student at Stanford University.